On the relationship between exposure to particles and dustiness during handling of powders in industrial settings

Ribalta C[1,2]., Viana M[1]., López-Lilao A[3]., Estupiñá S[3]., Minguillón M.C[1]., Mendoza J[4]., Díaz J[4]., Dahmann D[5]., Monfort. E[3].

[1]Institute of Environmental Assessment and Water Research (IDÆA-CSIC), C/ Jordi Girona 18, 08034 Barcelona, Spain.
[2]Barcelona University, Chemistry Faculty, C/ de Martí i Franquès, 1-11, 08028 Barcelona, Spain
[3]Institute of Ceramic Technology (ITC)- AICE - Universitat Jaume I, Campus Universitario Riu Sec, Av. Vicent Sos Baynat s/n, 12006 Castellón, Spain.
[4]Scientific and Technological Centres Barcelona University (CCiTUB), C/ Lluís Solé i Sabaris, 1-3, 08028 Barcelona, Spain
[5] Institut für Gefahrstoff-Forschung (IGF), Waldring 97, D 44789 Bochum, Germany.

Abstract

Exposure to ceramic powders, which is frequent during handling operations, is known to cause adverse health effects. Finding proxy parameters to quantify exposure is useful for efficient and timely exposure assessments. Worker exposure during handling of five materials (a silica sand (S1), three quartzes (Q1, Q2 and Q3) and a kaolin (K1)) with different particle shape (prismatic and platy) and sizes (3.4 - 120 μm) was assessed. Materials handling was simulated using a dry pendular mill under two different energy settings (low and high). Three repetitions of two kilos of material were carried out per material and energy conditions with a flow rate of 8 - 11 kg/h. The performance of the dustiness index as a predictor of worker exposure was evaluated correlating material's dustiness indexes (with rotating drum and continuous drop) with exposure concentrations. Significant impacts on worker exposure in terms of inhalable and respirable mass fractions were detected for all materials. Mean inhalable mass concentrations during background were always lower than 40 $\mu g/m^3$ whereas during material handling under high energy settings mean concentrations were 187, 373, 243, 156 and 430 $\mu g/m^3$ for S1, Q1, Q2, Q3 and K1 respectively. Impacts were not significant with regard to particle number concentration: background particle number concentrations ranged between 10620 – 46421 $/cm^3$ while during handling under high energy settings they were 20880 - 40498 $/cm^3$. Mean lung deposited surface area during background ranged between 27 - 101 $\mu m^2/cm^3$ whereas it ranged between 22 - 42 $\mu m^2/cm^3$ during materials handling. TEM images evidenced the presence of nanoparticles (≤ 100 nm) in the form of aggregates (300 nm - 1 μm) in the worker area, and a slight reduction on mean particle size during handling was detected. Dustiness and exposure concentrations showed a high degree of correlation (R^2 = 0.77 - 0.97) for the materials and operating conditions assessed, suggesting that dustiness could be considered a relevant predictor for workplace exposure. Nevertheless, the relationship between dustiness and exposure is complex and should be assessed for each process, taking into account not only material behaviour but also energy settings and workplace characteristics.

Keywords: indoor air, prediction of exposure, airborne dust, exposure assessment, particulate matter, industrial settings, nanoparticles

1. Introduction

Exposure to airborne particles is a growing field of research due to its complexity and intrinsic difficulty with regard to standardization. This is linked to the large variety of sources, processes and hazardous materials involved. The ceramic industry is a relevant case study, as it results in personal exposures in ambient and indoor air to a wide range of potentially hazardous raw materials and because during the manufacturing cycle a wide variety of bulk materials is used. In most cases, these materials are dry micro-sized (or even nano-sized) powders. As described by Brouwer et al. (2004), the aerosolization of submicrometer particles in workplaces is not limited to nanotechnology facilities. New technologies such as laser ablation, laser thermal treatment or inkjet printing, and green materials developments such as bactericidal and easy-clean surfaces, are currently being introduced in the traditional ceramic sectors (Gabaldón-Estevan et al., 2014; Llop et al., 2014; Monfort, 2012). The use of these new technologies as well as the growing and emerging markets represent new challenges in terms of occupational health (Fonseca et al., 2016; Fonseca et al., 2015; Viana et al., 2017; Voliotis et al., 2014).

Particulate matter (PM) as well as ultrafine particles (UFP) can penetrate deep in the human respiratory tract, the finest fractions reaching the alveolar region (Brunekreef & Forsberg, 2005; Pope & Dockery, 2006). Respiratory-related disease in the ceramic industry due to inhalable dust has already been reported (Alim et al., 2015; Dehghan et al., 2009; Neghab et al., 2009). In Spain, concentration limit values have been established for particulate matter exposure (not otherwise specified) as 10000 $\mu g/m^3$ and 3000 $\mu g/m^3$ for inhalable and respirable mass fractions, respectively (INSH, 2017).

The number of studies dealing with exposure is relatively low when compared with the wide variety of possible exposure scenarios in industrial settings (Brouwer et al., 2009). However, exposure assessment is a key component of risk assessment, which is generally combined with toxicological studies (Kuhlbusch et al., 2011). Thus, it is essential to determine exposure under different real world industrial scenarios as well as to predict exposure and establish efficient risk management strategies. In recent years many efforts were carried out to control and reduce exposure, although less attention was paid to the production processes and material handling (Lidén, 2006). In this framework, dustiness has risen as a valuable tool for occupational safety (Hamelmann & Schmidt, 2003), as it is a measure of a material's tendency to generate airborne dust during handling. However, discussions are ongoing about the use of the dustiness index as a direct predictor for worker exposure (Dubey et al., 2017; Fonseca et al., 2018) because dust emissions are known to depend on powder properties, the amount of material handled, the process, and local controls (Fransman et al., 2011). Certain authors (Brouwer, 2006; Class et al., 2001; Fonseca et al., 2018; Heitbrink et al., 1990) found no clear or limited relationship between exposure and dustiness, although they pointed out the importance of this parameter for risk assessment. On the other hand, Breum et al. (2003) despite finding a clear positive relation between dustiness and exposure, did not use their results for exposure prediction. Finally, some factors should be taken into account when establishing the relation between dustiness and exposure: 1) two standard methods are described in (EN 15051); 2) dustiness

depends mainly on material particle size distribution, humidity, density, morphology and specific surface area (SSA) (Hamelmann & Schmidt, 2003; Lidén, 2006; López-Lilao et al., 2016, 2015); and 3) dustiness tests should mimic as closely as possible the actual process energy applied (Evans et al., 2013). As a result, dustiness is currently used as an input for exposure modelling (Levin et al., 2014; Schneider and Jensen, 2007) and by materials producers to modify products in order to reduce dust generation (Lidén, 2006), rather than as a direct exposure predictor.

In this context, the present work aims to 1) assess exposure to airborne particles during handling of five highly used ceramic materials, paying special attention to material characteristics (size and particle shape) as well as to the influence of operating conditions (energy input); 2) assess dustiness indexes of the output materials to understand their emission mechanisms; and 3) correlate actual exposure concentrations with dustiness indexes, with the final goal to contribute on the understanding of the potential use of dustiness as a predictor of worker exposure.

2. Methodology

2.1. Experimental setup and instrumentation

The experiments took place in the pilot plant of the Institute of Ceramic Technology (ITC), Castellón, Spain during 4 days in October 2016. The pilot plant is divided into two connected rooms of 406 m^2 and 182 m^2 partly separated by a wall, which allows for air exchange at two different points (Figure 1). The plant is operated on a regular basis by 5 or more workers carrying out different activities. Material handling took place in room 1. The exterior door leading outdoors was kept open, as this is the plant's normal procedure.

Worker exposure to airborne particles was monitored during handling of powder materials during a process which included feeding of the materials to a dry pendular mill and extracting the powders from it. In order to study only handling (and not milling) emissions, a mill not altering the primary particle size but instead only modifying the size of the aggregates was selected, so that the process resembled the one that would occur during the handling operations. To verify this, the primary particle diameters of the input and output materials were determined by laser diffraction (wet method, see section 2.3) and no significant differences were observed. Modifying the primary particle size would have required additional mechanical action (Evans et al., 2013), which was not applied in this case. The mill selected for this purpose was a pilot-plant scale Poittemill PM-LB, with a nominal output capacity around 20 kg/h.

Particle mass, number concentration and alveolar lung deposited surface area (LDSA) were monitored as well as particle size distribution and morphological/chemical characterization. Three sampling locations were selected (Figure 1):

- Worker area: the devices were placed at a distance from the emission source similar to where the worker is standing (1 m from the floor and 50 cm from the emission source). The location is representative of the breathing zone, even if it may not be considered strictly as such. Devices used were: a butanol Condensation Particle

Counter (CPC, TSI Model 3775; sample flow rate 1.5 l/min) to measure particle number concentration (4 - 1500 nm, 1 minute time resolution); an electrical mobility spectrometer (NanoScan SMPS, TSI Model 3910; sample flow rate 0.7 l/min) to measure particle size distribution in 13 channels (10 - 420 nm, 1 minute time resolution); a miniature diffusion size classifier (DiSCmini Matter Aerosol, Testo; sample flow rate 1 l/min) to measure particle number concentration, mean particle size and lung deposited surface area (LDSA) (10 - 700 nm, 1 minute time resolution); and a Mini Laser Aerosol Spectrometer (Grimm, Mini-LAS 11R; sample flow rate 1.2 l/min) to measure particle mass concentration (0.25 - 32 μm, 31 channels, 1 minute time resolution). In addition, TEM grids (Qunatifolil ® Au grids with 1 μm diameter holes - 4 μm separation of 200 mesh) were placed in a sampling cassette (SKC INC., USA, inlet diameter 1/8 in. and filter diameter 25 mm) following the sampling setup described by Tsai et al., (2008). The Cassette was connected to a Leland pump (3 l/min). Sampling was performed in the worker area and indoor locations during handling for each material and for two energy settings of the pendular mill (low and high; see 2.2). Chemical and morphological analysis was later carried out by TEM J2100 coupled with an energy-dispersive X-ray (EDX) spectrometer.

- Indoor: a monitoring location inside the plant far from the processes of study but still connected by air flows. It was representative of the pilot plant's background concentrations. Devices used were a DiSCmini (see above) and a Mini Wide Range Aerosol Spectrometer (Mini-WRAS 1371; Grimm; sample flow rate 1.2 l/min) to measure particle mass concentration, particle number concentration and particle size distribution from 10 nm to 35 μm in 41 channels with a 1 minute time resolution. Additionally, TEM particle collection was carried out (see above).

- Outdoor: an outside monitoring location was set close to the main entrance of the plant. Devices used were a DiSCmini and a Grimm Mini-LAS (see above).

Indoor and outdoor monitoring points are not going to be extensively discussed. They are used mainly to discuss about indoor and outdoor influence over the worker area measurements.

All online instruments were time-synchronized and inter-compared overnight. Calibration of the Grimm laser spectrometers (Mini-LAS and Mini-WRAS) followed the procedures recommended by the manufacturer and are occasionally calibrated with regard to gravimetric reference samples. It should be noted that this kind of calibration is not carried out with the same aerosol as monitored in the present work, which would be the advisable procedure for any workplace exposure assessment (PD CEN/TR 16013 - 2:2010).

Devices started monitoring between 30 and 60 minutes before the start of the process (pre-activity), and the average results in this period before the process were used as a background particle concentration (Brouwer et al., 2009; Demou et al., 2008).

Worker area exposures were considered statistically significant when the following approach, described by Asbach et al. (2012) and Kaminski et al. (2015), was fulfilled:

Mean value during operation > BG + 3*(σBG)

where BG is the mean temporal background concentration (pre-activity) and σBG is the standard deviation of the background concentration.

2.2. Target materials, operations and conditions

Five different micronized materials, widely used in the ceramic industry, were selected (Table 1 and Table S1, Supporting information): Silica sand, S1 (d_{50} = 120 μm; CAS: 14940-68-2), three types of quartz, Quartz Q1, Quartz Q2 and Quartz Q3 (d_{50} 3.4 - 12.1 μm; CAS: 14808-60-7), and kaolin, K1 (d_{50} = 5.7 μm; CAS: 1332-58-7) sieved through a 5 mm mesh. Materials particle size distribution (d_{50}) determination was carried out by using laser diffraction; methodology described in more detail in section 2.3. According to the aspect ratio (AR) silica sand and quartz particles were considered to be prismatic (ca. spherical), while kaolin was platy (plate-like) shaped (micrographs of Q2 and K1, Figure S1, Supporting information). Because the moisture content of powders can affect material dustiness and exposure (Levin et al., 2015; Lidén, 2006) and also, due to pendular mill working requirements, all materials were previously dried using an oven at 105 - 110 ºC during at least 24h.

High energy (HE) (frequently used) and low energy (LE) operating conditions were tested, being representative for this industrial sector. Operating conditions are determined by air and material flow rate, aspiration intensity, milling speed and particle separation (Table 2).

Three repetitions were carried out for each material and condition. Approximately 2 kg of material were manually fed by the pilot plant worker into the mill grinding chamber for each repetition. All the materials were processed for 12 - 15 minutes (material flow 8 - 11 kg/h; Table 2), the exact time depending on how long it took for the material to be introduced in the mill's chamber due to its flowability. At the end of each repetition the output material was manually collected and stored for subsequent chemical and dustiness analysis.

Finally, cleaning operations were also monitored.

2.3. Materials characterisation

Input and output materials were characterized:

- Specific surface area (SSA) was assessed according to the BET method by nitrogen absorption (Brunauer et al., 1928).

- Materials flowability was assessed by using the Hausner ratio (HR); the quotient of the bulk density of the packed particle bed (by tapping) and the aerated bulk density of the particle bed, obtained by dropping powder into a container without stirring or vibration. In this regard, where the bigger the HR the lower the followability (Mallol et al., 2008).

- Particle Size Distribution (PSD) was determined by laser diffraction (d_{laser}) wet method (ISO 13320-1, 2009) using the Mastersizer 2000 that analyse the sample by the theory of Fraunhofer and Mie with a size resolution of 0.02 - 2000 μm and by and X-ray gravitational sedimentation using the Sedigraph method from Micrometrics (d_{stokes}).

- The aspect ratio (AR), a particle shape factor defined as the ratio of the particle's major dimension and minor dimension, was determined by the Parslow-Jennings method for oblate spheroids (Jennings & Parslow, 1988; Otterstedt & Brandreth, 2013). This method is based on the fact that d_{laser} and $d_{sedigraph}$ (previously described) have different dependence on aspect ratio and, therefore, we can only obtain the same diameter in the case of spherical particles.

$$\frac{d_{stokes}}{d_{laser}} = \sqrt{\frac{2\,.\,AR.\arctan\sqrt{(AR^2-1)}}{AR.\sqrt{(AR^2-1)+\ln\left[AR+\sqrt{(AR^2-1)}\right]}}} \quad (1)$$

where AR is the aspect ratio, d_{stokes} the diameter of a sphere with the same density and setting velocity as the particle of interest (μm), and d_{laser} is the diameter of the sphere of same diameter as the cross-sectional projection of the particle (μm).

This factor is a measure of the irregularity of particle shape, i.e. deviation from a spherical shape. For prismatic, platy, and ribbon-like particles the aspect ratios were 1 - 5, 4 - 15, and 5 - 100, respectively (Otterstedt & Brandreth, 2013). Therefore, the selected quartzes and sands can be considered prismatic particles and the kaolin can be classified as platy or ribbon-like particle.

In addition, airborne particles collected on Au Quantifoil ® grids during handling were morphologically and chemically characterised by TEM-EDX (Markowicz & Grieken, 2001; Williams & Carter, 2009).

2.4. Dustiness tests

Dustiness tests were performed for all materials and conditions (high and low energy) tested, before and after the handling process (input and output materials). The two dustiness tests described by the EN 15051 (2013) (Continuous drop method; López-Lilao et al., 2016), and rotating drum method (Pensis et al., 2009) were performed following the standard, although with only two repetitions/material (Figure S2, Supporting information).

2.5. Statistical analysis and data treatment

Log-normality and homogeneity were assessed with the Shapiro-Wilk and Levene's test, respectively and, as data did not fulfil normality assumptions, the non-parametric Mann-Whitney "U" Test was performed in order to determine statistically significant differences between mean airborne particle diameters measured with the NanoScan.

3. Results and Discussion

3.2. Exposure assessment

Mean background concentrations (pre-activity) for the inhalable fraction were below 40 μg/m^3 for all the materials except for S1 (92.1 μg/m^3) and Q1 (58.9 μg/m^3) (Table 3). Outdoor, indoor and background concentrations for $PM_{2.5}$ were representative of $PM_{2.5}$ outdoor concentrations (20 - 30 μg/m^3; Pérez et al., 2008). Outdoor air to indoor micro-

sized particle concentration was deemed negligible (Figure S3, Supporting information).

As expected, particle mass concentrations in the worker area, for all the materials, increased during handling (Table 3, Figure 2 and S4, Supporting information). Previous studies have already seen impacts on dust concentrations in both particle number and mass during material handling on paint factories pouring (Koivisto et al., 2015; Koponen et al., 2015), during bag filling of black carbon production (Kuhlbusch, et al., 2004), and during weighing bulk CNTs and sanding epoxy containing CNTs (Cena & Peters, 2011). Particle mass concentrations, for all repetitions, showed a marked cycle that consisted on a peak during material feeding and then a decrease, showing a clear impact on coarse particles due to handling for high and low energy settings (Figure 2 and S4, Supporting information). Mean inhalable mass concentrations during low energy settings were 189.5, 80.8, 106.8 and 319.1 μg/ m^3 for Q1, Q2, Q3 and K1 respectively whereas during high energy settings they were 373.0, 243.6, 156.0 and 429.6 μg/ m^3 (Table 3). Koponen et al. (2015) also described cyclic behaviour for materials pouring, with a concentration peak at the beginning of the activity. Hence, in some cases the number of repetitions can be more critical than the amount of material processed and thus the repetitions (start and stop) of a process is a factor that should be taken into account for exposure assessment models (Koponen et al., 2015). The time-weighted averages (TWA) for exposure levels are shown in Table S2, Supporting information. The highest value for the inhalable mass fraction was 429.6 μg/m^3 during K1 handling. This is well below the inhalable (10000 μg/m^3) and respirable (3000 μg/m3) OELs (INSH, 2017). Additional information regarding the calculation of the TWAs is provided in Table S2 (Supporting information).

On the contrary, the impact of handling on fine particles, measured with the CPC, was lower than for micro-sized particles. The trend observed for particle number concentration during handling suggests a more cumulative trend than for mass, especially for high energy conditions (Figure 2 and Figure S4, Supporting information). However, a significant increase in mean number concentration was not observed for any of the materials except for S1. This was probably due to the more frequent coagulation/adsorption processes of ultrafine particles onto coarse particles, which resulted in lower particle number concentrations. Recommended exposure concentrations during handling were not exceeded in any case, again with the exception of S1 which was on the limit of 40000 /cm^3 (Van Broekhuizen et al., 2012). Alveolar lung deposited surface area, monitored with DiSCmini (Table 3) was seen to decrease during materials handling when compared with pre-activity values (background). Mean LDSA during background concentrations ranged between 27.1 - 100.9 $\mu m^2/cm^3$ whereas during materials handling they ranged between 22.1 - 42.3 $\mu m^2/cm^3$.

Concerning mill cleaning operations, the highest 1-min peak concentrations for nano- and micro-sized particles when considering background + handling + cleaning were recorded during the cleaning operation, specifically during vacuuming (Figure 2 and S4, and Table S3, Supporting information). The maximum 1-min peak recorded during the cleaning operation for inhalable mass fraction of material Q1 was 13824 μg/m^3. Regarding particle number concentrations, maximum 1-min peak concentrations of 81247, 64443 and 77385 /cm^3 were recorded for Q2, Q3 and K1 (materials with lower

d_{50}), respectively (Table S3, Supporting information). On the other hand, mean concentrations during cleaning were higher than the corresponding background concentrations for both inhalable and respirable mass fractions and for all materials except S1. However, there is no significant increase of mean number concentration for any of the materials when comparing with their respective background concentrations.

Yeganeh et al. (2008) observed an increase of $PM_{2.5}$ during a similar sweeping operation of a fullerenes production reactor, while an increase in number concentration was also not observed, which is consistent with our results. On the other hand, Demou et al. (2008) detected increases in particle number concentration during reactor cleaning operations, especially when vacuuming (maxim of 50000 /cm^3), identifying the vacuuming operation as an important short-term source of particles during cleaning. Other authors such as Fujitani et al. (2008) and Maynard et al. (2004) also reported the influence of vacuuming on particle number concentration and although the particle source is not clear, two main hypotheses were established by Maynard et al. (2004): (1) particle increase is due to materials aerosolization or (2) particles are generated on the unit's carbon brush motor, which seems to be the most probable reason in this case. In the present study, the maximum 1-min peaks recorded during the cleaning operation coincided with vacuuming, supporting the results of the previous studies despite differences in materials, processes and devices used.

Additionally, a case study regarding the use of a general ventilation system as a potential mitigation strategy in the pilot plant has been assessed and it is described in the Supporting information (Figure S5, Supporting information).

3.2.1. Material differences and influence of operating conditions

Generally particle mass concentrations increased when energy setting was set from low to high except for material Q1 (which decreased from 70.7 μg/m^3 under low energy settings to 48.0 μg/m^3 under high energy settings) (Figure 3, Table 3). For the inhalable mass fraction, significant increases with respect to the background concentrations were found during handling with high energy conditions (Figure 3b) for all materials, except for S1, ranging from 4.6 to 33.1 times the background concentrations. Contrarily, for low energy settings (Figure 3a), a significant increase was only seen for K1 (24.6 times higher than the background concentration), and in general, increases when comparing with the background values were lower than when using high energy conditions. When using high energy, increases between 25.7 to 66.8% in inhalable mass concentrations were found comparing with low energy concentrations. Jensen et al. (2015) tested two different working styles (careful and careless) for sanding of glass- and carbon fibre-reinforced composites, and found increases in particle concentrations between 1.1 and 14.1% when working in the careless style compared with careful working style. Results from Jensen et al. (2015) and the ones herein suggest that operating conditions play an important role on worker exposure concentrations and therefore should be always considered when implementing corrective measures as well as for exposure prediction. On the other hand, the material with the highest inhalable mass exposure was K1 (platy shaped; mean particle diameters of 5.7 μm and highest SSA) followed by Q1 and Q2 (both prismatic, c.a. spherical) with mean particle diameter of 12.1 and 5.8 μm, respectively and with the lowest SSA values. Thus, no clear relationship between

exposure concentrations and particle size, SSA or shape could be identified with the samples monitored.

Regarding the respirable mass fraction, significant increases were found when using high energy conditions for Q2, Q3, K1 and S1 (Figure 3d). On the other hand, when using low energy conditions, the respirable mass fraction only showed a significant increase for Q2 and K1 (Figure 3c). Again, also for respirable mass concentrations, higher exposure values were observed under high energy settings. The two materials with higher exposure concentrations for low and high energy settings were K1 and Q2, respectively, both with material particle d_{50} around 5 μm (Table 1), but K1 with platy shape and Q2 prismatic. Various authors (López-Lilao et al., 2016, 2015; Pensis et al., 2009; Upton et al., 1990) reported that materials emission patterns do not follow a linear correlation with particle size, and that the assumption that finer materials have higher emissions is not always true. Materials with high content of ultrafine particles and comparably narrow size distribution have high cohesive forces and as a consequence material dustiness is lower than that of materials with a relatively larger mean particle diameter but with low ultrafine particles content. These materials show higher dustiness given that cohesive forces are less strong and ultrafine particles are easily released.

In general, particle number concentrations did not show an increase with respect to the background (pre-activity), except for S1, which was the only material showing a significant increase probably due to sources other than handling (Figure 2, 4 and S4, Supporting information). The presence of ultrafine particles from various sources is frequent in industrial settings (Viitanen et al., 2017). On the other hand, when comparing low and high energy settings, particle number concentration for all the prismatic (c.a. spherical) materials increased with the energy settings while it decreased for the platy (plate-like) shaped material K1 (from 24002 to 20880 /cm^3) (Figure 4, Table 3). Contrarily to what happened with the mass fractions, K1 is the material showing the lowest particle number concentration (Figures 3 and 4). Thus, for the materials and conditions assessed, handling of powder materials did not generate statistically significant emissions in terms of particle number concentrations.

However, results presented in Figures 5 and 6 indicate that handling may have had an impact on the mean size of the emitted ultrafine particles. This is supported by the TEM images in Figure 7 (see section 3.2.3). According to Figure 5, for S1, Q2, Q3 and K1, when using high energy conditions, mean particle size underwent a statistically significant reduction compared to background mean particle sizes (reductions in diameter in the order of 12 - 43%). However, interferences from other processes may have influenced this decrease for the S1 material (43% decrease). Under low energy conditions this influence was lower, as the reduction was only statistically significant for 2 materials. It may be hypothesised that handling allowed the release of the smaller particles contained in the materials due to aggregates breaking. Further work would be necessary to confirm this hypothesis.

When assessing the particle size distribution (Figure 6, instead of the mean diameter in Figure 5), results show only slight differences during background (pre-activity), and handling (low and high energy conditions). For Q1, Q3 and K1 materials, a slight dominance of finer particles was seen compared to during background, where the size

distribution was dominated by coarser particles. Only during S1 a clear increase of particles under 30 nm was observed (probably due to interferences from other processes, as stated above).

3.2.3. Exposure characterization – TEM and EDX analysis

TEM images of the sampled particles during handling were analysed in order to characterise the emitted particles (Figure 7; the EDX analyses are shown in Figure S6, Supporting Information). Particles during handling under high energy conditions of S1 were mainly formed by Si, Al, and Fe showing a compact structure (Figure 7a and S6a, Supporting information). Aside from this, large nanoparticle aggregates (main element C) were also detected suggesting the contamination by another process (a furnace being switched on or even diesel soot from outdoor air, e.g., Figure 7b, 7c and Figure S6b, Supporting information). This was also the case for materials Q2, Q3 and K1 (Figures 7i, 7l, 7o and Figure S6h S6k and S6n, Supporting information). Particles observed in Q1, Q2 and Q3 samples were mainly SiO_2 particles (0.5 - 2 μm, < 1 μm and 200 nm respectively) (Figures 7d, 7e, 7f, 7g, 7h and 7k, and S6c, S6d, S6e, S6f, S6g and S6j, Supporting information). However, smaller particles (< 100 nm) were also observed in form of aggregates (Figure 7g, 7j, 7k 7n and S6f, S6i, S6j, Supporting information). For K1, aggregates of particles < 500 nm (main elements: Si, Fe, O and Ca) presenting a platy shape were observed (Figure 7m, 7n, S6l and S6m, Supporting information). This analysis supports the conclusion extracted above whereby it was observed that, while micron-scale particles dominated emissions during handling, nano-scaled particles forming aggregates were also emitted and may potentially impact worker exposure.

3.3. Comparison between dustiness and exposure concentrations

Materials dustiness index was assessed for Q1, Q2, Q3 and K1 materials after being handled under low and high energy settings (Table 1). In addition, for high energy conditions the material S1 was also included using the continuous drop method. Dustiness concentrations are usually provided in terms of inhalable and/or respirable mass fraction using mg/kg as units. Inhalable dustiness results were then correlated with inhalable mass fraction exposure concentrations during handling (Figure 8) aiming to assess the potential ability of the dustiness index to predict exposure concentrations.

Inhalable dustiness indexes obtained ranged between 463 and 10012 mg/kg for the continuous drop method, and 64 and 410 mg/kg for the rotating drum. K1 and Q1 were the materials showing higher dustiness indexes followed by Q2 and Q3, (Table 1, Figure 8). The lowest dustiness value was found for S1. Pensis et al. (2009) reported that dustiness is dependent on material nature as well as d_{50}. Moreover, López-Lilao et al. (2016) concluded, after examining quartz dustiness, that for quartzes with d_{50} < 25 μm an increase of mean particle size corresponds to an increase of dustiness while for quartzes with d_{50} > 25 μm the opposite effect takes place. Taking this into account, the results in Table 1 and Figure 8 seem to agree with those findings, with Q1 having the highest dustiness of the three analysed quartzes. According to the literature, significant correlations may be observed between particle SSA and dustiness when comparing different quartzes (López-Lilao et al., 2016) and different kaolin samples (López-Lilao et al., 2015). Previous works (López Lilao et al., 2017) have shown that, for

approximately spherical and dry materials, coarser mean diameters present a higher potential for release of fine particles. Thus, dustiness depends on the amount of fine particles and the material's ability to release such fine particles. However, dustiness does not only depend on particle SSA and establishing a relationship between these parameters is complex (Pensis et al., 2009; Plinke et al., 1995, 1992). In addition, in Evans et al. (2013), where dustiness of different fine and nanoscale powders was analysed, no correlation between SSA and dustiness was found, suggesting that primary particle size, in their specific case, was not the key factor when determining material dustiness. Thus, it is evident that the current literature presents contradicting results. The present study shows that the highest exposure concentrations and dustiness indexes were measured for materials with very different SSA values (e.g., kaolin (K1) and quartz (Q1), 9.6 and 1.4 m^2/g respectively) and different particle shapes (e.g., platy kaolin and prismatic quartz). These results confirm the difficulty to establish a general relationship between dustiness and materials physical-chemical characteristics.

As shown in Figure 8, R^2 correlation values dustiness – exposure ranged between 0.77 and 0.97 when using the inhalable fraction for both energy settings and dustiness methods. The best correlation was obtained for the continuous drop method with the low energy settings (R^2 = 0.97); contrarily, the worst correlation was obtained for the rotating drum method with low energy settings (R^2 = 0.77). For high energy settings, correlations obtained were R^2 0.83 and 0.88 for continuous drop and rotating drum method, respectively. The results indicate that continuous drop can reproduce slightly better what happened under low energy handling settings and rotating drum can reproduce better the processes taking place under high energy handling settings given that materials suffer a similar process inside the rotating drum than inside the mill. The continuous drop method uses fresh material continuously whereas the rotating drum method does not, and the material in the continuous drop is just falling and being resuspended with air flow while in the rotating drum method the material suffers rotating forces. Thus, it can be expected that both methods provide different results. Pensis et al. (2009) evaluated both EN dustiness methods and studied the correlation between them when using the inhalable and respirable fractions, and found weak correlations between methods for both mass fractions. However, here a strong correlation between methods (continuous drop and rotating drum) was found when considering the inhalable fraction (R^2 = 0.78; data not shown).

Results obtained herein regarding dustiness – exposure correlations suggest that dustiness could be considered a predictor of exposure for the materials and particle sizes tested. Other authors have previously reported good exposure – dustiness correlations. Heitbrink et al. (1989) found significant correlations between two dustiness testers and worker exposure during bag packing. Breum et al. (2003) also found good correlation between exposure during installation of cellulosic fibres and rotating drum dustiness results. Contrarily, Class et al. (2001) found limited correlation of exposure during manufacturing of insulation wools and ceramic fibres with the dustiness shaking box test, as well as Brouwer et al. (2006), who found a correlation of 0.70 between rotating drum dustiness values and worker exposure during sweeping/cleaning and scooping/weighing/adding. Finally, some other authors did not find a clear correlation as it the case of Heitbrink et al. (1990) who reported very limited correlation, and only

good correlation after some adjustments during bag dumping and filling. Recently, Fonseca et al. (2018) did also not find a clear correlation during laboratory spilling of nano-scaled materials with mini-rotating drum dustiness results. To come to the point, no clear relationship dustiness – exposure has yet been clearly stablished so that dustiness could be used as a direct predictor of worker exposure. However, dustiness is one of the parameters frequently included in equations for exposure prediction (Levin et al., 2014; Schneider et al., 2011) although prediction modelling for particulate matter is not always as precise as expected (Fonseca et al., 2017; Koivisto et al., 2015). Thus, it is important to continue working on modelling, dustiness test performance as well as to understand which are the key factors to predict worker exposure.

4. Conclusions

Personal exposure during handling of 5 different powder materials, as well as material dustiness, were assessed and compared in a real-world industrial setting in the ceramic industry. Particles between 4 nm and 32 μm were monitored in terms of number and mass concentration. Results evidence that handling of powder materials had a significant impact on exposure in terms of particle mass, and that this impact was larger under high energy settings: the mean inhalable mass fraction under low energy settings 80.8 - 319.1 $\mu g/m^3$, and 156.0 - 429.6 $\mu g/m^3$ under high energy settings. Therefore, the modification of the energy settings can be an effective mitigation strategy for this kind of process. On the contrary, emissions in terms of particle number concentrations (mean particle number concentration during handling 15033 – 40498 $/cm^3$) were not significant (pre-activity concentrations = 10620 – 46421 $/cm^3$). However, the assessment of the particle diameter plus the analysis of TEM images evidenced the release of nanoparticles to workplace air and that these nanoparticles may have a potential impact on worker exposure. Dustiness indexes were calculated for all the materials assessed with the two standard methods (continuous drop and rotating drum). A high degree of correlation between dustiness and exposure concentrations was found during handling (R^2 = 0.77 -0.97), for inhalable mass fraction and for low (R^2 = 0.77 - 0.97) and high (R^2 = 0.83 - 0.88) energy settings. These results suggest that dustiness may be considered a relevant predictor of workplace exposure for the materials, particle sizes, energy settings and dustiness methods evaluated. Proxy parameters such as dustiness for exposure characterisation may be useful tools to deliver timely and efficient exposure assessments. However, due to this parameter's complexity, the relationship between dustiness and exposure should be assessed for each industrial processes taking into account operational settings as well as materials physical-chemical properties and workplace characteristics.

5. Acknowledgements

This research was founded by the Spanish MINECO (CGL2015-66777-C2-1-R, 2-R), Generalitat de Catalunya AGAUR 2014 SGR33, the Spanish Ministry of the Environment (13CAES006) and FEDER (European Regional Development Fund) "Una manera de hacer Europa". M.C. Minguillón acknowledges the Ramón y Cajal Fellowship awarded by the Spanish Ministry of Economy, Industry and

Competitiveness. The authors also acknowledge the company MOLARIS for their support with technical information on the mill used. The authors declare no conflict of interest relating to the material presented in this Article.

6. References

Alim, M. A., Biswas, M. K., Biswas, G., Hossain, M. A., & Ahmad, S. A. (2015). Respiratory health problems among the ceramic workers in Dhaka. *Faridpur Medical College Journal*, *9*(1), 19. http://doi.org/10.3329/fmcj.v9i1.23617

Asbach, C., Kuhlbusch, T. A. J., Kaminski, H., Stahlmecke, B., Plitzko, S., Götz, U., … Dahmann, D. (2012). Standard Operation Procedures For assessing exposure to nanomaterials, following a tiered approach.

Breum, N. O., Schneider, T., Jørgensen, O., Rasmussen, T. V., & Skibstrup Eriksen, S. (2003). Cellulosic Building Insulation versus Mineral Wool, Fiberglass or Perlite: Installer's Exposure by Inhalation of Fibers, Dust, Endotoxin and Fire-retardant Additives. *Ann. Occup. Hyg*, *47*(8), 653–669. http://doi.org/10.1093/annhyg/meg090

British Standards Institute. (2009). Particle size analysis — Laser diffraction methods, BS ISO 13320-1:1999.

Brouwer, D. H., Gijsbers, J. H. J., & Lurvink, M. W. M. (2004). Personal Exposure to Ultrafine Particles in the Workplace: Exploring Sampling Techniques and Strategies. *Annals of Occupational Hygiene*, *48*(5), 439–453. http://doi.org/10.1093/annhyg/meh040

Brouwer, D. H., Links, I. H. M., De Vreede, S. A. F., & Christopher, Y. (2006). Size selective dustiness and exposure; simulated workplace comparisons. *Annals of Occupational Hygiene*, *50*(5), 445–452. http://doi.org/10.1093/annhyg/mel015

Brouwer, D., Van Duuren-Stuurman, B., Berges, M., Jankowska, E., Bard, D., & Mark, D. (2009). From workplace air measurement results toward estimates of exposure–Development of a strategy to assess exposure to manufactured nano-objects. *Journal of Nanoparticle Research*, *11*(8), 1867–1881. http://doi.org/10.1007/s11051-009-9772-1

Brunauer, S., Emmert, P. H., & Teller, E. (1928). Adsorption of gases in multimolecular layers. J. Am. Chem. Soc, 60, 309-319. *Journal of the American Chemical Society*, 309–319.

Brunekreef, B., & Forsberg, B. (2005). Epidemiological evidence of effects of coarse airborne particles on health. *European Respiratory Journal*, *26*(2), 309–318. http://doi.org/10.1183/09031936.05.00001805

Cena, L. G., & Peters, T. M. (2011). Characterization and Control of Airborne Particles Emitted During Production of Epoxy/Carbon Nanotube Nanocomposites. *Journal of Occupational and Environmental Hygiene*, *8*(2), 86–92. http://doi.org/10.1080/15459624.2011.545943

Class, P., Deghilage, P., & Brown, R. C. (2001). Dustiness of different high-temperature insulation wools and refractory ceramic fibres. *Annals of Occupational Hygiene*, *45*(5), 381–4.

Dehghan, F., Mohammadi, S., Sadeghi, Z., & Attarchi, M. (2009). Respiratory Complaints and Spirometric Parameters in Tile and Ceramic Factory Workers.

Tanaffos, *8*(4), 19–25.

Demou, E., Peter, P., & Hellweg, S. (2008). Exposure to manufactured nanostructured particles in an industrial pilot plant. *Annals of Occupational Hygiene*, *52*(8), 695–706. http://doi.org/10.1093/annhyg/men058

Dubey, P., Ghia, U., & Turkevich, L. A. (2017). Computational fluid dynamics analysis of the Venturi Dustiness Tester. *Powder Technology*, *312*, 310–320. http://doi.org/10.1016/j.powtec.2017.02.030

European Committee for Standardization (CEN). (2013). *Workplace exposure: Measurement of the dustiness of bulk materials; Part1: Requirements and choice of test methods; Part 2: Rotating drum method; Part 3: Continuous drop method (EN 15051). [Stantdard] Brussels, Belgium, 2013*.

Evans, D. E., Turkevich, L. A., Roettgers, C. T., Deye, G. J., & Baron, P. A. (2013). Dustiness of fine and nanoscale powders. *Annals of Occupational Hygiene*, *57*(2), 261–277. http://doi.org/10.1093/annhyg/mes060

Fonseca, A. S., Koivisto, A. J., Koponen, I. K., Jensen, A. C. Ø., Kling, K. I., Levin, M., ... Jensen, K. A. (2017). Goodness of dustiness index for predicting human exposure to airborne nanomaterials. *In New Tools and Approaches for Nanomaterial Safety Assessment - Book of Abstracts [#1552] Malaga, Spain.* Retrieved from http://orbit.dtu.dk/files/128854576/BOOK_OF_ABSTRACTS.pdf

Fonseca, A. S., Kuijpers, E., Kling, K. I., Levin, M., Koivisto, A. J., Nielsen, S. H., … Koponen, I. K. (2018). Particle release and control of worker exposure during laboratory-scale synthesis, handling and simulated spills of manufactured nanomaterials in fume hoods. *Journal of Nanoparticle Research*, *20*(2). http://doi.org/10.1007/s11051-018-4136-3

Fonseca, A. S., Maragkidou, A., Viana, M., Querol, X., Hämeri, K., de Francisco, I., … de la Fuente, G. F. (2016). Process-generated nanoparticles from ceramic tile sintering: Emissions, exposure and environmental release. *Science of The Total Environment*, *565*, 922–932. http://doi.org/10.1016/j.scitotenv.2016.01.106

Fonseca, A. S., Viana, M., Querol, X., Moreno, N., de Francisco, I., Estepa, C., & de la Fuente, G. F. (2015). Ultrafine and nanoparticle formation and emission mechanisms during laser processing of ceramic materials. *Journal of Aerosol Science*, *88*, 48–57. http://doi.org/10.1016/j.jaerosci.2015.05.013

Fransman, W., Van Tongeren, M., Cherrie, J. W., Tischer, M., Schneider, T., Schinkel, J., … Tielemans, E. (2011). Advanced Reach Tool (ART): Development of the Mechanistic Model. *Annals of Occupational Hygiene*, *55*(9), 957–79. http://doi.org/10.1093/annhyg/mer083

Fujitani, Y., Kobayashi, T., Arashidani, K., Kunugita, N., & Suemura, K. (2008). Measurement of the Physical Properties of Aerosols in a Fullerene Factory for Inhalation Exposure Assessment. *Journal of Occupational and Environmental Hygiene*, *5*(6), 380–389. http://doi.org/10.1080/15459620802050053

Gabaldón-Estevan, D., Criado, E., & Monfort, E. (2014). The green factor in European manufacturing: A case study of the Spanish ceramic tile industry. *Journal of Cleaner Production*, *70*, 242–250. http://doi.org/10.1016/j.jclepro.2014.02.018

Hamelmann, F., & Schmidt, E. (2003). Methods of Estimating the Dustiness of Industrial Powders – A Review. *KONA Powder and Particle Journal*, *21*(March),

7–18. http://doi.org/10.14356/kona.2003006

Heitbrink, W. A., Todd, W. F., & Fischbach, T. J. (1989). Correlation of tests for material dustiness with worker exposure from the bagging of powders. *Applied Industrial Hygiene*, *4*(1), 12–16. http://doi.org/10.1080/08828032.1989.10389884

Heitbrink, W. A., Tood, W. F., Cooper, T. C., & O'Brien, D. M. (1990). The Application of Dustiness Tests to the Prediction of Worker Dust Exposure. *American Industrial Hygiene Association Journal*, *51*(4), 217–223. http://doi.org/10.1080/15298669091369565

INSH. (2017). *LEP 2017*. *Instituto Nacional de Seguridad e Higiene en el Trabajo.* http://doi.org/10.1017/CBO9781107415324.004

Jensen, A. C. Ø., Levin, M., Koivisto, A. J., Kling, K. I., Saber, A. T., & Koponen, I. K. (2015). Exposure assessment of particulate matter from abrasive treatment of carbon and glass fibre-reinforced epoxy-composites – Two case studies. *Aerosol and Air Quality Research*, *15*(5), 1906–1916. http://doi.org/10.4209/aaqr.2015.02.0086

Jennings, B.R., and K. Parslow. (1988). Particle size measurement: the equivalent spherical diameter.. *Proceedings of the Royal Society of London A*, 419. p.137–149

Kaminski, H., Beyer, M., Fissan, H., Asbach, C., & Kuhlbusch, T. A. J. (2015). Measurements of nanoscale TiO2 and Al2O3 in industrial workplace environments – Methodology and results. *Aerosol and Air Quality Research*, *15*(1), 129–141. http://doi.org/10.4209/aaqr.2014.03.0065

Koivisto, A. J., Jensen, A. C. Ø., Levin, M., Kling, K. I., Maso, M. D., Nielsen, S. H., … Koponen, I. K. (2015). Testing the near field/far field model performance for prediction of particulate matter emissions in a paint factory. *Environ. Sci.: Processes Impacts*, *17*(1), 62–73. http://doi.org/10.1039/C4EM00532E

Koponen, I. K., Koivisto, A. J., & Jensen, K. A. (2015). Worker exposure and high time-resolution analyses of process-related submicrometre particle concentrations at mixing stations in two paint factories. *Annals of Occupational Hygiene*, *59*(6), 749–763. http://doi.org/10.1093/annhyg/mev014

Kuhlbusch, T. A., Asbach, C., Fissan, H., Göhler, D., & Stintz, M. (2011). Nanoparticle exposure at nanotechnology workplaces: A review. *Particle and Fibre Toxicology*, *8*(1), 22. http://doi.org/10.1186/1743-8977-8-22

Kuhlbusch, T. A. J., Neumann, S., & Fissan, H. (2004). Number Size Distribution, Mass Concentration, and Particle Composition of PM_{1}, $PM_{2.5}$, and PM_{10} in Bag Filling Areas of Carbon Black Production. *Journal of Occupational and Environmental Hygiene*, *1*(10), 660–671. http://doi.org/10.1080/15459620490502242

Levin, M., Koponen, I. K., & Jensen, K. A. (2014). Exposure Assessment of Four Pharmaceutical Powders Based on Dustiness and Evaluation of Damaged HEPA Filters. *Journal of Occupational and Environmental Hygiene*, *11*(3), 165–177. http://doi.org/10.1080/15459624.2013.848038

Levin, M., Rojas, E., Vanhala, E., Vippola, M., Liguori, B., Kling, K. I., … Jensen, K. A. (2015). Influence of relative humidity and physical load during storage on dustiness of inorganic nanomaterials: implications for testing and risk assessment. *Journal of Nanoparticle Research*, *17*(8), 337. http://doi.org/10.1007/s11051-015-

Lidén, G. (2006, July). Dustiness testing of materials handled at workplaces. *Annals of Occupational Hygiene*. http://doi.org/10.1093/annhyg/mel042

Llop et al., 2014. (2014). The Ceramic Industry in Spain: Challenges and Opportunities in Times of Crisis. Retrieved from http://repositori.uji.es/xmlui/handle/10234/123013

López-Lilao, A., Bruzi, M., Sanfélix, V., Gozalbo, A., Mallol, G., & Monfort, E. (2015). Evaluation of the Dustiness of Different Kaolin Samples. *Journal of Occupational and Environmental Hygiene*, *12*(8), 547–554. http://doi.org/10.1080/15459624.2015.1019079

López-Lilao, A., Escrig, A., Orts, M. J., Mallol, G., & Monfort, E. (2016). Quartz dustiness: A key factor in controlling exposure to crystalline silica in the workplace. *Journal of Occupational and Environmental Hygiene*, *13*(11). http://doi.org/10.1080/15459624.2016.1183011

López Lilao, A., Sanfélix Forner, V., Mallol Gasch, G., & Monfort Gimeno, E. (2017). Particle size distribution: A key factor in estimating powder dustiness. *Journal of Occupational and Environmental Hygiene*, *14*(12), 975–985. http://doi.org/10.1080/15459624.2017.1358818

Mallol, G., Amorós, J. L., Orts, M. J., & Llorens, D. (2008). Densification of monomodal quartz particle beds by tapping. *Chemical Engineering Science*, *63*(22), 5447–5456. http://doi.org/10.1016/j.ces.2008.07.032

Markowicz, A. A., & Grieken, R. E. Van. (2001). *Handbook of X-Ray Spectrometry*. Marcel Dekker.

Maynard, A. D., Baron, P. A., Foley, M., Shvedova, A. A., Kisin, E. R., & Castranova, V. (2004). Exposure to Carbon Nanotube Material: Aerosol Release During the Handling of Unrefined Single-Walled Carbon Nanotube Material. *Journal of Toxicology and Environmental Health, Part A*, *67*(1), 87–107. http://doi.org/10.1080/15287390490253688

Monfort, E. (2012). What tole do ceramic tiles play in green procurement and sustainable building? *In: Qualicer 2012 - World Congress on ceramic tile quality* (pp. 1–22). Retrieved from http://www.qualicer.org/recopilatorio/ponencias/pdfs/2012167.pdf

Neghab, M., Zadeh, J. H., & Fakoorziba, M. R. (2009). Respiratory toxicity of raw materials used in ceramic production. *Industrial Health*, *47*(1), 64–9. Retrieved from http://www.ncbi.nlm.nih.gov/pubmed/19218759

Otterstedt, J. E., & D. A., Brandreth. (2013). Small particles technology. *Springer Science & Business Media.*

PD CEN/TR 16013-2:2010 - Workplace exposure. Guide for the use of direct-reading instruments for aerosol monitoring. Evaluation of airborne particle concentrations using optical particle counters. (n.d.).

Pensis, I., Mareels, J., Dahmann, D., & Mark, D. (2009). Comparative Evaluation of the Dustiness of Industrial Minerals According to European Standard EN 15051, 2006. *Annals of Occupational Hygiene*, *54*(2), 204–16. http://doi.org/10.1093/annhyg/mep077

Pérez, N., Pey, J., Querol, X., Alastuey, A., López, J. M., & Viana, M. (2008). Partitioning of major and trace components in PM10-PM2.5-PM1 at an urban site in Southern Europe. *Atmospheric Environment*, *42*(8), 1677–1691. http://doi.org/10.1016/j.atmosenv.2007.11.034

Petavratzi, E., Kingman, S. W., & Lowndes, I. S. (2007). Assessment of the dustiness and the dust liberation mechanisms of limestone quarry operations. *Chemical Engineering and Processing: Process Intensification*, *46*(12), 1412–1423. http://doi.org/10.1016/j.cep.2006.11.005

Plinke, M. A. E., Leith, D., Boundy, M. G., & Löffler, F. (1995). Dust Generation from Handling Powders in Industry. *American Industrial Hygiene Association Journal*, *56*(3), 251–257. http://doi.org/10.1080/15428119591017088

Plinke, M. A. E., Maus, R., & Leith, D. (1992). Experimental examination of factors that affect dust generation by using Heubach and MRI testers. *American Industrial Hygiene Association Journal*, *53*(5), 325–330. http://doi.org/10.1080/15298669291359726

Pope, C. A., & Dockery, D. W. (2006). Health Effects of Fine Particulate Air Pollution: Lines that Connect. *Journal of the Air & Waste Management Association*, *56*(6), 709–742. http://doi.org/10.1080/10473289.2006.10464485

Schneider, T., Brouwer, D. H., Koponen, I. K., Jensen, K. A., Fransman, W., Van Duuren-Stuurman, B., … Tielemans, E. (2011). Conceptual model for assessment of inhalation exposure to manufactured nanoparticles. *Journal of Exposure Science and Environmental Epidemiology*, *21*(5), 450–463. http://doi.org/10.1038/jes.2011.4

Schneider, T., & Jensen, K. A. (2007). Combined Single-Drop and Rotating Drum Dustiness Test of Fine to Nanosize Powders Using a Small Drum. *Annals of Occupational Hygiene*, *52*(1), 23–34. http://doi.org/10.1093/annhyg/mem059

Tsai, S.-J., Ashter, A., Ada, E., Mead, J. L., Barry, C. F., & Ellenbecker, M. J. (2008). Airborne Nanoparticle Release Associated with the Compounding of Nanocomposites using Nanoalumina as Fillers. *Aerosol and Air Quality Research*, *x*(x).

Upton, S., Hall, D., & Marsland, G. (1990). Some experiments on material dustiness. *Aeorosol Society Annual Conference, University of*. Retrieved from https://scholar.google.com/scholar_lookup?publication_year=1990&pages=325-330&issue=5&author=S.L.+Uptonauthor=D.J.+Hallauthor=G.W.+Marsland&title=Some+experiments+on+material+dustiness

Van Broekhuizen, P., Van Veelen, W., Streekstra, W. H., Schulte, P., & Reijnders, L. (2012). Exposure limits for nanoparticles: Report of an international workshop on nano reference values. *Annals of Occupational Hygiene* (Vol. 56, pp. 515–524). Edinburgh Napier University,. http://doi.org/10.1093/annhyg/mes043

Viana, M., Fonseca, A. S., Querol, X., López-Lilao, A., Carpio, P., Salmatonidis, A., & Monfort, E. (2017). Workplace exposure and release of ultrafine particles during atmospheric plasma spraying in the ceramic industry. *Science of The Total Environment*, *599*, 2065–2073. http://doi.org/10.1016/j.scitotenv.2017.05.132

Viitanen, A. K., Uuksulainen, S., Koivisto, A. J., Hämeri, K., & Kauppinen, T. (2017). Workplace measurements of ultrafine particles-A literature review. *Annals of Work Exposures and Health*. http://doi.org/10.1093/annweh/wxx049

Voliotis, A., Bezantakos, S., Giamarelou, M., Valenti, M., Kumar, P., & Biskos, G. (2014). Nanoparticle emissions from traditional pottery manufacturing. *Environmental Science: Processes & Impacts*, *16*(6), 1489. http://doi.org/10.1039/c3em00709j

Williams, D. B., & Carter, C. B. (2009). The Transmission Electron Microscope. In *Transmission Electron Microscopy* (pp. 3–22). Boston, MA: Springer US. http://doi.org/10.1007/978-0-387-76501-3_1

Yeganeh, B., Kull, C. M., Hull, M. S., & Marr, L. C. (2008). Characterization of airborne particles during production of carbonaceous nanomaterials. *Environmental Science and Technology*, *42*(12), 4600–4606. http://doi.org/10.1021/es703043c

Figures and Tables

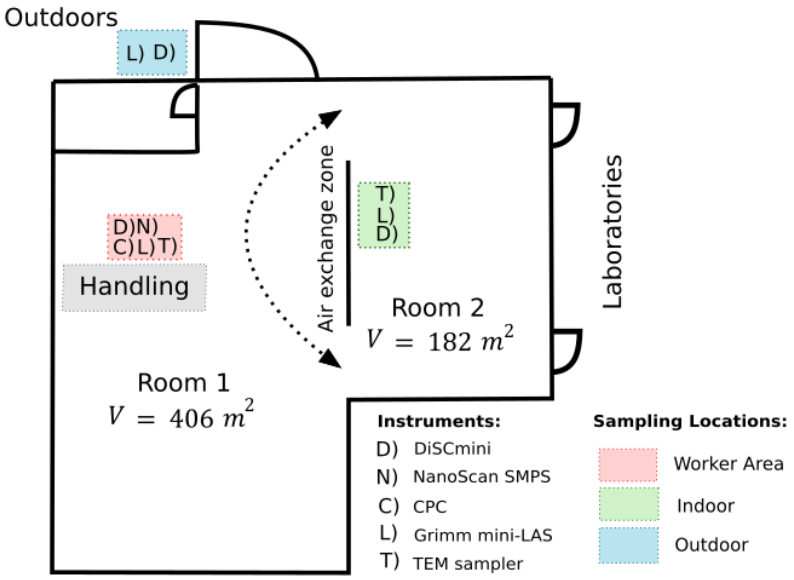

Figure 1. ITC pilot plant layout. Monitoring locations as well as devices used during the handling process are indicated.

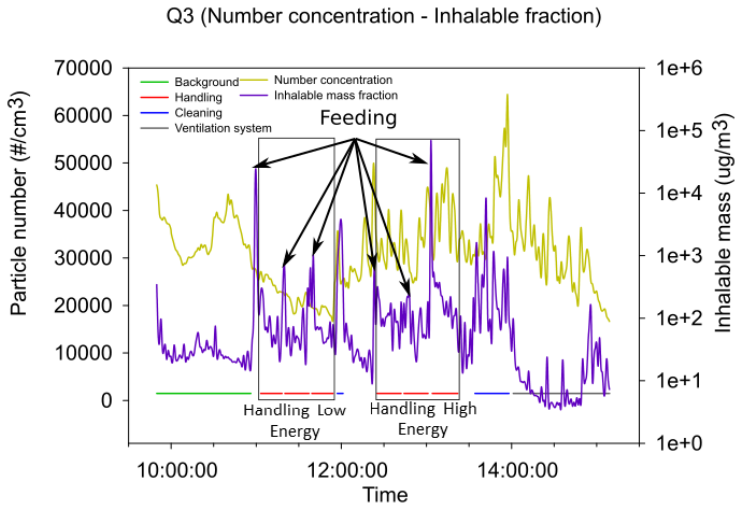

Figure 2. Time series of particle number concentration (monitored with CPC) and inhalable mass fraction in log scale (monitored with mini-LAS) for the Q3 material. Background, exhaust, cleaning and handling repetitions for low and high energy settings are marked on the bottom of the graph.

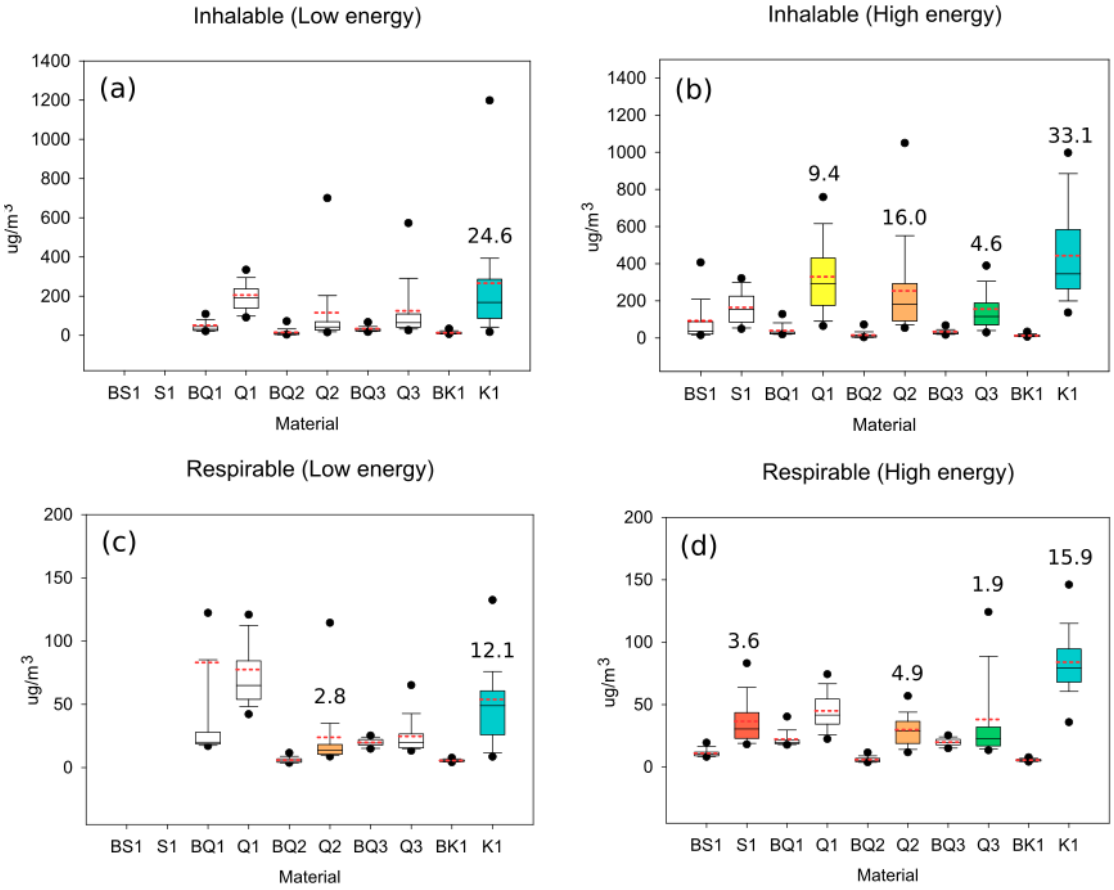

Figure 3. Vertical box plots for the inhalable and respirable mass fractions of the five materials during handling with high and low energy settings with each respective background concentration (pre-activity). The boundary of the box closest to zero indicates the 25th percentile and the farthest from zero the 75th percentile. The line within the box indicates the median value. Red dotted line within the box indicates the mean value. Error bars above and below indicates the 10th and 90th percentiles. Coloured box indicates statistically significant differences when comparing with its respective background concentration. Numbers on the top of each box indicate the increase comparing with its corresponding background concentration (only when statistically significant differences were detected).

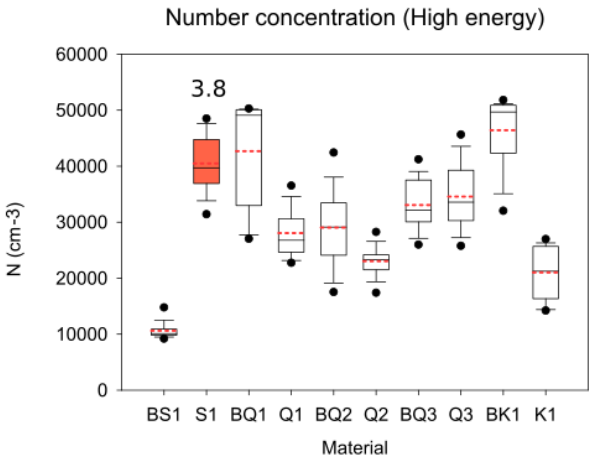

Figure 4. Vertical box plot for particle number concentrations of the five materials during handling with high energy settings and each respective background concentration (pre-activity). The boundary of the box closest to zero indicates the 25th percentile and the farthest from zero the 75th percentile. The line within the box indicates the median value. Red dotted line within the box indicates the mean value. Errors bars above and below indicates the 10th and 90th percentiles. Coloured box indicate significant differences when comparing with each background concentration. Values on the top of each box indicate the increase comparing with its corresponding background concentration (only when statistically significant differences were detected).

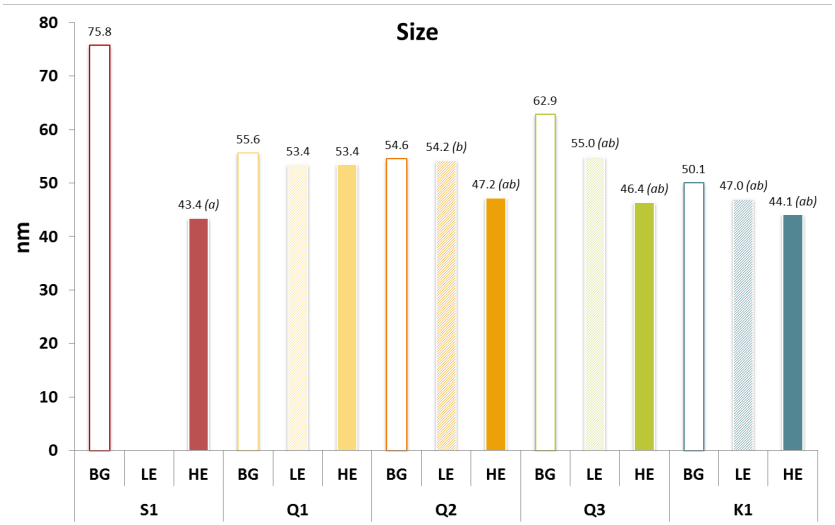

Figure 5. Mean particle diameter, as measured with the NanoScan in the worker area for the background period and during handling under low and high energy settings and for the five study materials. Letters in italics on the top of the bars indicate *(a)* significant differences between handling conditions (low and high energy settings) with respect to its background mean particle size and *(b)* significant differences between low and high energy settings mean particle size. The non-parametric Mann-Whitney "U" test was used to test statistically significant differences. Mean particle size differences between materials were not tested.

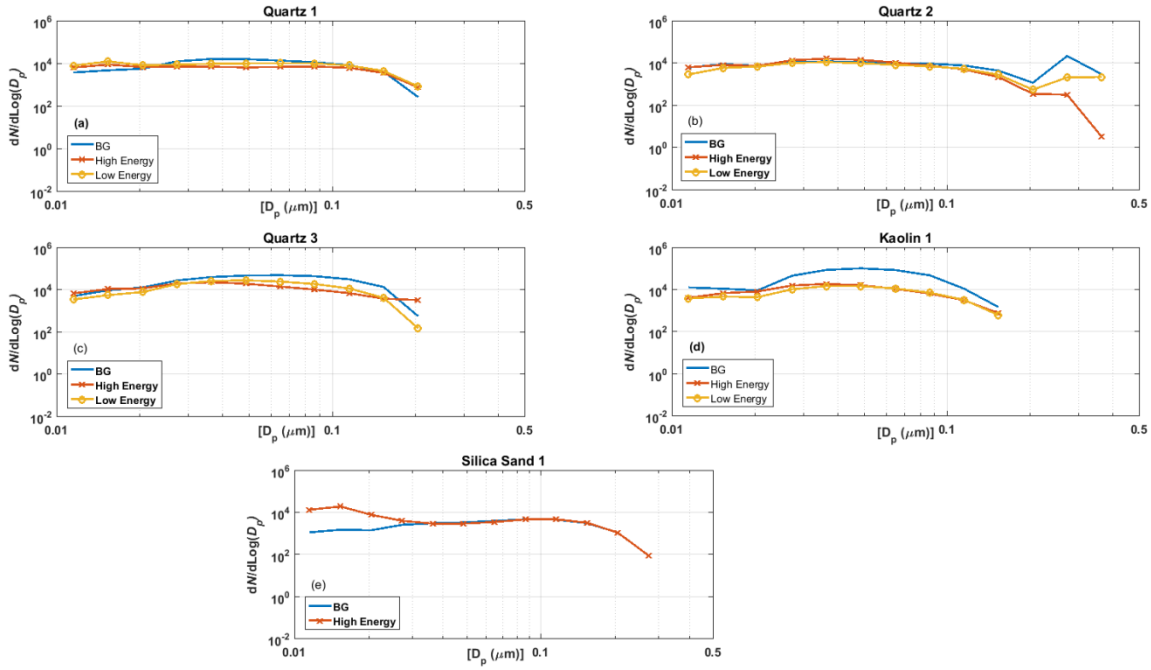

Figure 6. Particle number size distribution in the worker area (monitored with NanoScan) during handling under low and high energy settings, and during background conditions.

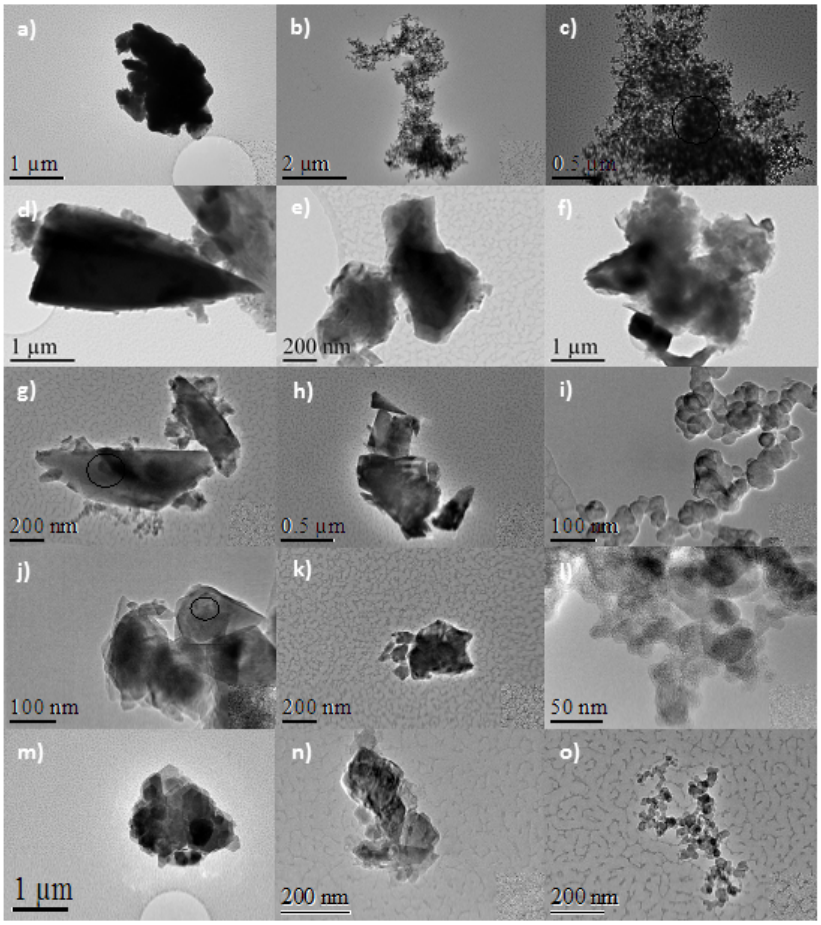

Figure 7. TEM images obtained from the worker area during handling of S1 (images a, b and c), Q1 (images d, e and f), Q2 (images g, h and i), Q3 (images j, k and l) and K1 (images m, n and o) when using high energy settings. a) main elements Fe, Si, Al; b) agglomerate of C nanoparticles; c) agglomerate of C nanoparticles; d) SiO_2 particle; e) agglomerate of SiO_2 particles; f) SiO_2 with other elements; g)

agglomerate of SiO_2 particles; h) SiO_2 particles with smaller ones surrounding; i) nanoparticles (main elements: K, C and Na); j) aggregates of SiO_2 ultrafine particles; k) SiO_2 particle (mean diameter 200 nm) with smaller ones surrounding it (mean diameter <100 nm); l) nanoparticles (main elements: C, Na); m) agglomerate of particles (main elements: Si, Al and O) with mean particle diameter < 500 nm; n) agglomerates of particles of different compositions (translucid particles: Si, Fe, O and Ca, darker particles: Ca and O); and o) nanoparticles (main element: C).

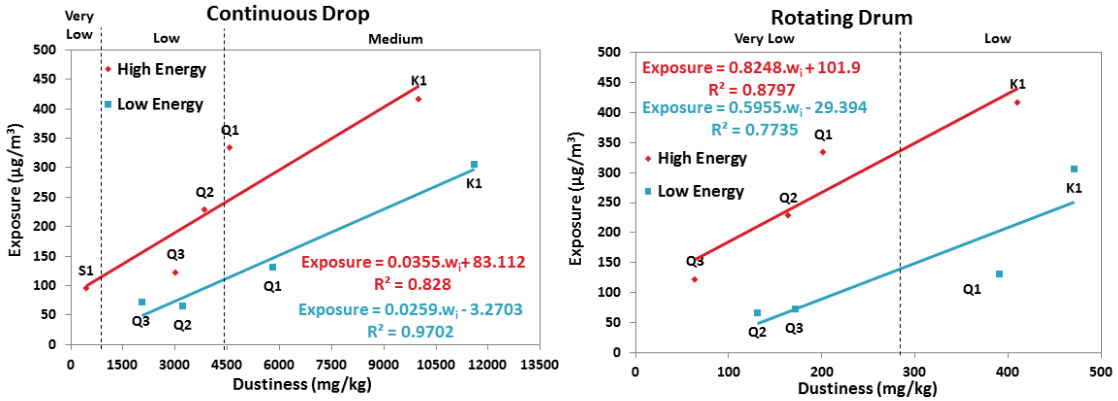

Figure 8. Correlation between exposure concentrations during handling and dustiness (inhalable mass fraction) using Q1, Q2, Q3 and K1. S1 was only used for high energy settings and with the continuous drop method due to availability issues. a) Continuous drop dustiness test b) Rotating drum dustiness test. Dustiness index classification values according to EN 15051 for each method is shown (dotted bars).

Table 1. Material type, material code, particle shape and most common uses in the ceramic industry are given. Particle size distribution: PSD in terms of di: diameter below which lies i% by volume of total particles, specific surface area: SSA, hausner ratio: HR and aspect ratio: AR are described for each material. Inhalable mass fraction and classification level are shown for the two dustiness methods (continuous drop and rotating drum). Moisture of all the samples before the start of the manipulation process was < 0.5%.

Material type	Code	Shape	Uses	d_{50} (µm)	d_{10} (µm)	d_{90} (µm)	SSA (m^2/g)	HR	AR	w_i (mg/kg) C.D	w_i (mg/kg) R.D
Zirconium silica sand	S1	Prismatic	Ceramics production	120	NDA	NDA	NDA	1.12	4.3	463 (Very Low)	NDA
Quartz	Q1	Prismatic	Materials preparation, forming, glazing or firing	12.1	1.4	37.0	1.4	1.64	3.3	4593 (Moderate)	202 (Very Low)
Quartz	Q2	Prismatic	Pigment production for the colouration of glazes	5.8	1.1	18.8	2.7	1.52	5.7	3855 (Low)	164 (Very Low)
Quartz	Q3	Prismatic	Used in rubber compounds	3.4	1.0	8.4	4.4	1.57	3.8	3029 (Low)	64 (Very Low)
Kaolin caobar	K1	Platy (plate-like) or ribbon-like	Traditional ceramics production. Cement and metallurgical industries	5.7	1.4	15.7	9.6	1.83	20	10012 (Moderate)	410 (Low)

Table 2. Milling parameters for low and high energy settings are described, aspiration intensity, mill speed and particle separation. Material process flow rate, for both energy settings, are also described.

Operating condition	Air flow rate (m^3/h)	Material flow rate (kg/h)	Milling speed (rpm)	Particle separation (rpm)
Low Energy	1600	8-11	1200	600
High Energy	1800	8-11	2250	1800

Table 3. Mean particle number, mass concentration and LDSA during handling of the powders at low and high energy settings. NDA: no data available.

		Low Energy Conditions				High Energy Conditions			
Material	Measurement point	Particle number (#/cm^3)	LDSA ($\mu m^2/cm^3$)	Inhalable fraction ($\mu g/m^3$)	Respirable fraction ($\mu g/m^3$)	Particle number (#/cm^3)	LDSA ($\mu m^2/cm^3$)	Inhalable fraction ($\mu g/m^3$)	Respirable fraction ($\mu g/m^3$)
S1	Background	NDA	NDA	NDA	NDA	10620 (9179-16431)	NDA	92.1 (14.6-1168.3)	11.0 (7.7-20.1)
	Worker area	NDA	NDA	NDA	NDA	**40498 (30713-49155)**	NDA	187.2 (57.7-454.8)	**39.1 (18.4-105.9)**
Q1	Background	24439 (19249-29660)	46.1 (29.8-156.3)	58.9 (20.3-599.2)	20.9 (16.0-52.6)	42686 (25421-51461)	48.2 (28.8-69.4)	39.6 (19.0-299.8)	22.2 (17.3-91.1)
	Worker area	30310 (24624-36399)	30.8 (27.5-40.4)	189.5 (76.0-337.0)	70.7 (40.6-126.9)	28059 (22427-40300)	22.1 (18.4-27.2)	**373.0 (126.2-1074.1)**	48.0 (22.5-89.7)
Q2	Background	29036 (15904-47210)	27.1 (20.7-43.6)	15.2 (3.8-135.1)	5.9 (3.6-15.7)	29036 (15904-47210)	27.1 (20.7-43.6)	15.2 (3.8-135.1)	5.9 (3.6-15.7)
	Worker area	15033 (10149-23264)	22.7 (17.0-40.5)	80.8 (11.8-1660.5)	**16.9 (7.7-122.5)**	23091 (16805-30928)	26.9 (20.5-31.1)	**243.6 (61.7-1069.3)**	**29.3 (11.7-83.9)**
Q3	Background	33064 (24959-43430)	100.9 (68.1-132.6)	34.1 (15.0-343.6)	19.9 (13.1-32.7)	33064 (24959-43430)	100.9 (68.1-132.6)	34.1 (15.0-343.6)	19.9 (13.1-32.7)
	Worker area	21756 (17223-35332)	42.3 (29.1-59.7)	106.8 (22.1-1031.7)	22.9 (12.0-68.6)	34214 (24961-48730)	39.1 (28.5-168.0)	**156.0 (21.0-1052.8)**	**37.9 (12.0-331.9)**
K1	Background	46421 (30470-53894)	72.6 (43.2-104.5)	13.0 (5.8-34.7)	5.5 (4.0-8.0)	46421 (30470-53894)	72.6 (43.2-104.5)	13.0 (5.8-34.7)	5.5 (4.0-8.0)
	Worker area	24002 (15419-49458)	22.8 (18.2-35.2)	**319.1 (70.6-1705.3)**	**66.8 (25.6-370.9)**	20880 (14149-26659)	27.3 (16.8-39.9)	**429.6 (136.0-999.3)**	**87.4 (58.6-162.0)**

Supporting Information:

On the relationship between exposure to particles and dustiness during handling of powders in industrial settings

Ribalta C[1,2]., Viana M[1]., López-Lilao A[3]., Estupiñá S[3]., Minguillón M.C[1]., Mendoza J[4]., Díaz J[4]., Dahmann D[5]., Monfort. E[3].

Contents:

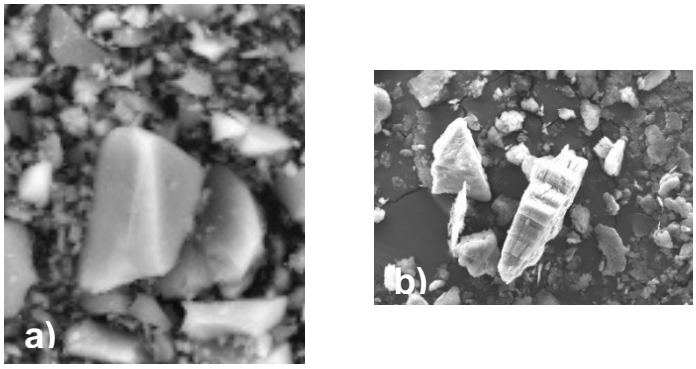

Figure S1. Micrographs of the original materials. a) Q2 and b) K1.

Method

Rotating drum

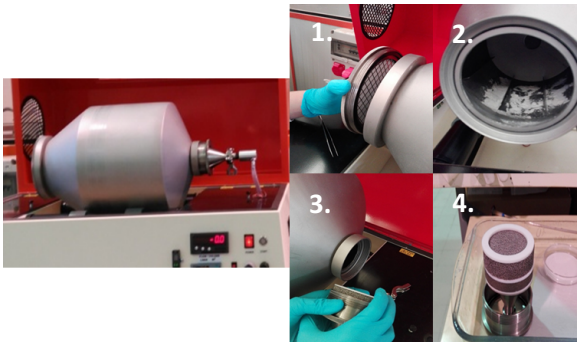

1. Inlet
2. Dust generation section (drum)
3. Dust collection
4. Foams and filter

Continuous drop

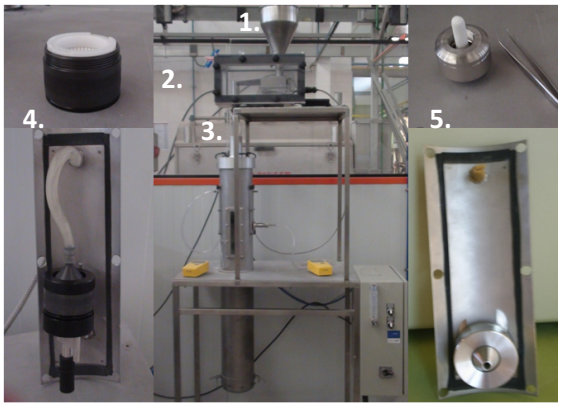

1. Sample tank
2. Metering device
3. Drop pipe
4. Sampling head for the respirable aerosol fraction
5. Sampling head the inhalable aerosol fraction

Figure S2. Pictures and description of the dustiness methods used, rotating drum and continuous drop.

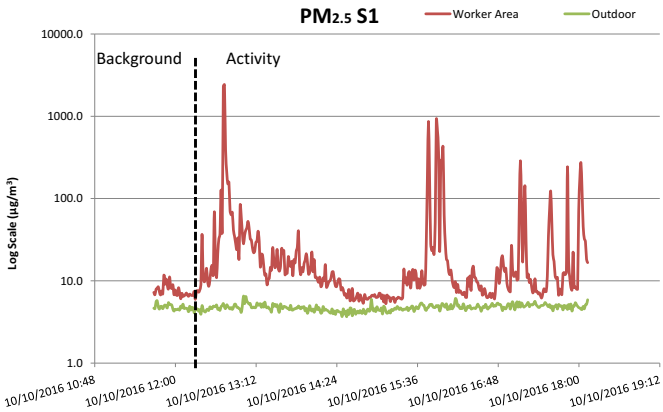

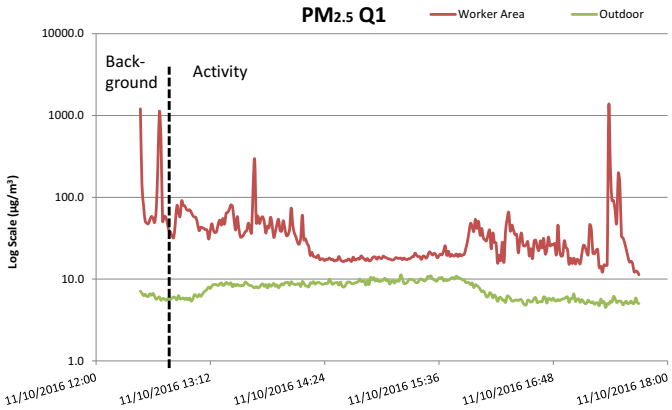

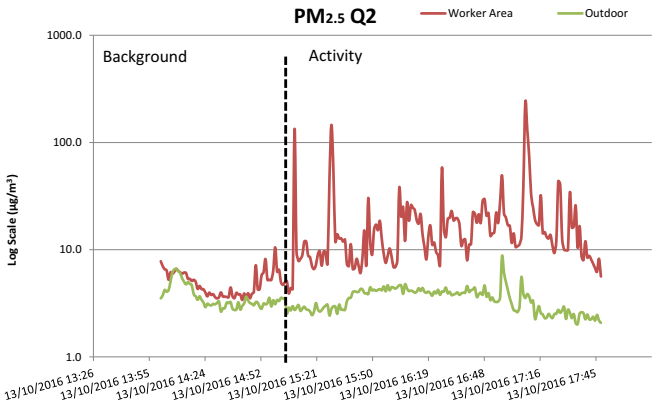

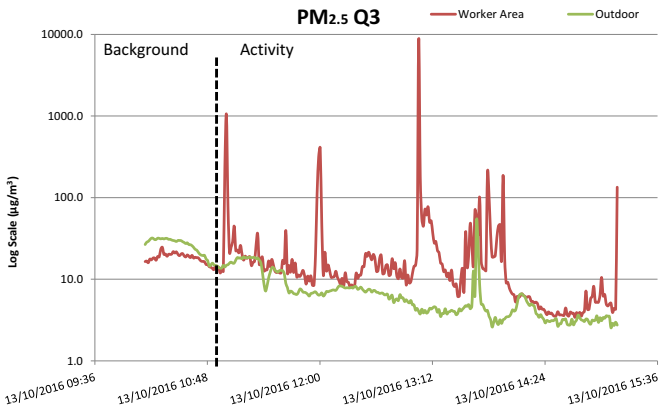

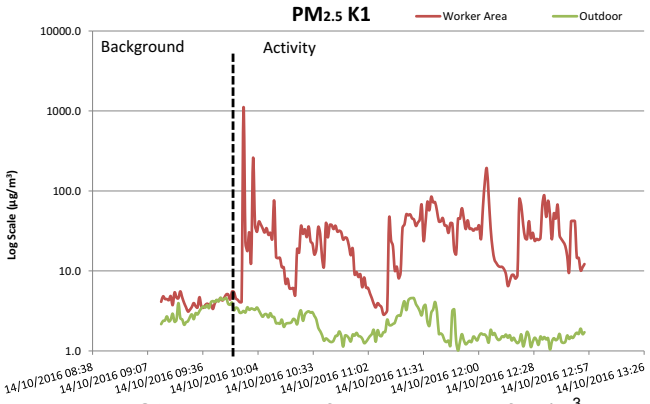

Figure S3. Time series of $PM_{2.5}$ in terms of µg/m^3 monitored with Grimm on the worker area and the outdoor measurement points for the materials S1, Q1, Q2, Q3 and K1. Note that the Y axis is in log scale. Worker Area is represented in red and outdoor in green. Background and activity periods are divided with a dotted black line.

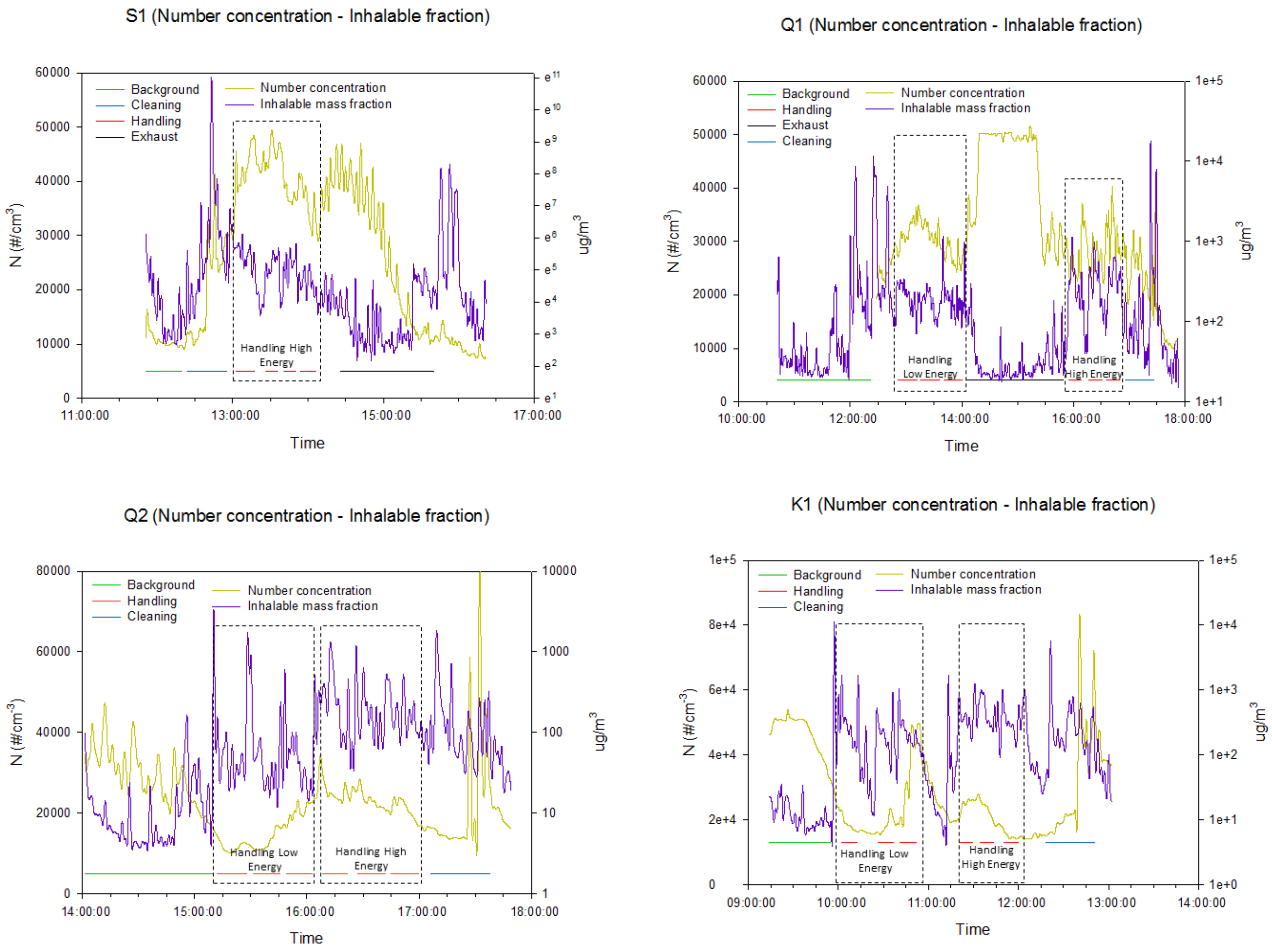

Figure S4. Time series of particle number concentration (monitored with CPC) and inhalable mass fraction in log scale (monitored with Grimm) for S1, Q1, Q2 and K1 materials. Background, exhaust, cleaning and handling repetitions for low and high energy settings are marked with colour bars at the bottom of the each graph (green, black, blue and red respectively). The three first red lines correspond to low energy settings and the last three ones to the high energy settings.

Potential mitigation strategies – Case study

The general room air extraction system was tested as a potential mitigation measure. Particle number and mass concentrations were then monitored. The extraction system was used three of the four days of the sampling campaign during approximately one hour during midday, when no other processes were ongoing. Figures 2 and S3 show that during when the air extraction system of the room was ON there was reduction of the inhalable mass fraction (coarse particles) as well as the respirable fraction. Other studies such as Cena and Peters, (2011); Douwes et al. (2017) and Jensen et al. (2015) also pointed out the relevance of the exhaust ventilation system on the removal of particles, although they used a local exhaust system. Contrarily, ultrafine particle concentrations during the time when the room air extraction system was ON did not decrease, and they even increased during one day (when Q1 material was assessed, Figure 2 and Figure S1). Mean and maximum particle number concentrations during the time when room extraction system was ON were 42686 and 51461 #/cm^3, respectively. Figure S1 shows the particle size distribution in the worker area for materials S1 and Q1. In both cases the highest concentrations for particles in the range

20 – 50 nm were reached during the time when the air extraction system was ON. For the first day (10/10/2016 – S1 material) the increasing trend in nanoparticles concentration started minutes before the extraction system was switched ON, while for the second day (11/10/2016 – Q1) the increase in nanoparticles concentration was produced during the air extraction system period. The particle size range monitored, from 20 to 50 nm, points to outdoor road traffic emissions as the source of these particles, as this is the typical size range of these emissions (Brines et al., 2015) and the main door of the plant was open all the time during the tests. Therefore, the air extraction system showed a clear decrease in coarse particle concentrations, but did not favour ultrafine particle reduction.

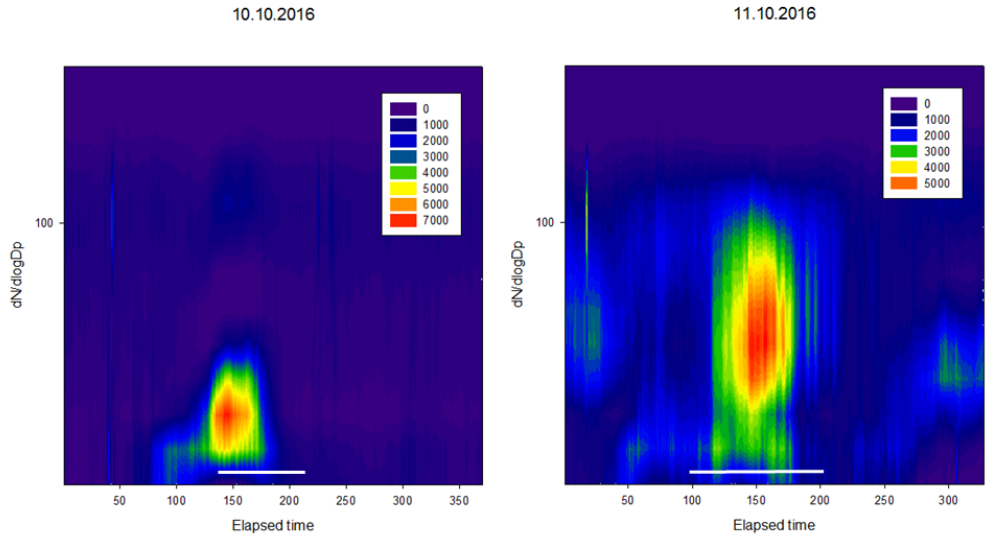

Figure S5. Particle size distribution (particle range from 10 to 420 nm) measured with the NanoScan for two of the sampling days 10/10/2016 and 11/10/2016, corresponding to materials S1 and Q1 respectively. Extraction system periods are marked with a white line under. Note that the particle number concentration colour scale is different for each graph.

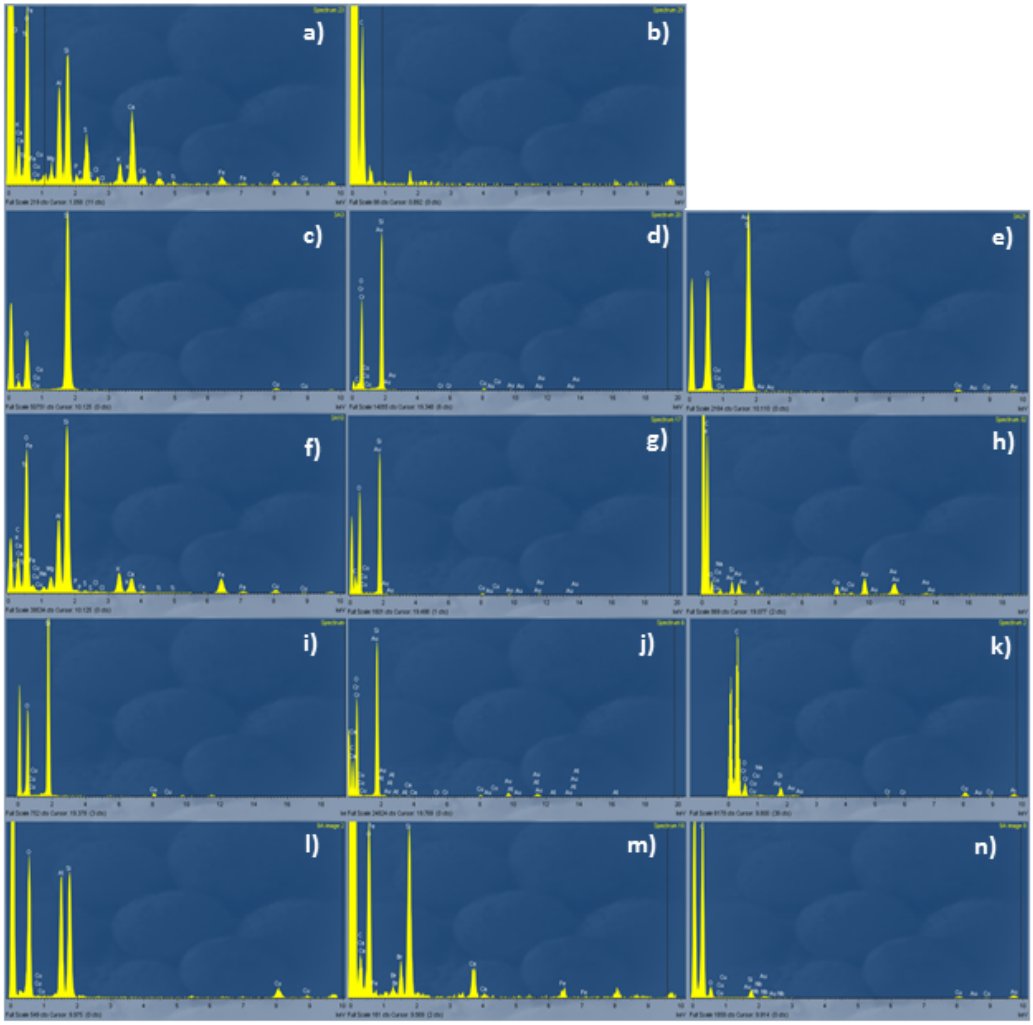

Figure S6. EDX spectrum analysis for TEM images presented in figure 7. EDX images correspond a) to 7a; b) to 7b and 7c; c) to 7d; d) to 7e; e) to 7f; f) to 7g; g) to 7h; h) to 7i; i) to 7j; j) to 7k; k) to 7l; l) to 7m; m) to 7n; n) to 7o.

Table S1. Materials chemical composition. Note: sand chemical composition was proportioned by the supplier.

Material	S1	Q1	Q2	Q3	K1
LOI 1050°C	NDA	0.3	0.63	0.40	12.8
SiO_2	32	99	98.4	99.6	49.1
Al_2O_3	NDA	0.60	0.80	0.02	36.7
TiO_2	NDA	0.03	0.06	0.01	0.11
Fe_2O_3	NDA	0.03	0.04	0.01	0.42
CaO	NDA	0.08	0.09	0.01	0.11
MgO	NDA	0.01	0.02	< 0.01	0.09
K_2O	NDA	0.1	0.07	0.01	0.59
Na_2O	NDA	0.01	< 0.01	< 0.01	0.03
ZrO_2	65	-			-

Table S2. TWA results for all materials and for inhalable and respirable mass fractions. For each material, temporal background concentrations, handling under low energy settings and handling under high energy settings are used for the calculation. TWA xh (µg/m^3): worker exposure during all the measurements period including temporal background, handling under low energy and under high energy settings. Note there are different sampling periods for each material. TWA 8h (µg/m^3): worker exposure using the temporal background concentrations to complete the 8h TWA. Limit values: inhalable 10000 µg/m^3 and respirable 3000 µg/m^3. Equation used:

$$TWA = \frac{t_1.c_1 + t_2.c_2 + \cdots\ t_n.c_n}{t_1 + t_2 + \cdots\ t_n}$$

where: c_n is the mean concentration during a specific operation and t_n is the time of the specific operation.

Material	**S1**		**Q1**		**Q2**		**Q3**		**K1**	
TWA_{xh} / TWA_{8h}	**$TWA_{2.5h}$** (µg/m^3)	**TWA_{8h}** (µg/m^3)	**$TWA_{4.1h}$** (µg/m^3)	**TWA_{8h}** (µg/m^3)	**$TWA_{3.5h}$** (µg/m^3)	**TWA_{8h}** (µg/m^3)	**$TWA_{3.6h}$** (µg/m^3)	**TWA_{8h}** (µg/m^3)	**TWA_{3h}** (µg/m^3)	**TWA_{8h}** (µg/m^3)
Inhalable fraction	591.4	256.5	242.2	152.8	134.4	67.4	626.2	295.6	267.9	107.5
Respirable fraction	106.9	42.6	56.9	39.4	24.3	14.0	139.7	72.8	51.6	22.6

Table S3. Mean particle number and mass concentration (inhalable and respirable fraction) in the worker area during cleaning operations for each material and their respective background concentrations. Statistically significant differences found after applying the exposure > 3σ+BG are marked in bold.

Material	**Number concentration Background**	**Number concentration Cleaning**	**Inhalable mass Background**	**Inhalable mass Cleaning**	**Respirable mass Background**	**Respirable mass Cleaning**
S1	10620 (9179-16431)	9869 (7615-12995)	92.1 (14.6-1168.3)	33.2 (15.2-74.8)	11.0 (7.7-20.1)	12.5 (8.5-20.6)
Q1	42686 (25420-51461)	24176 (17865-35288)	39.6 (19.0-300.0	**624.1 (26.4-13824.2)**	22.2 (17.3-91.1)	**123.8 (15.0-2384.3)**
Q2	29226 (16645-47210)	22153 (13591-81248)	15.2 (3.8-135.1)	**205.3 (31.8-1672.8)**	5.9 (3.6-15.7)	**52.7 (14.2-427.7)**
Q3	33064 (24959-43430)	42131 (30647-64444)	34.1 (15.0-343.6)	**662.1 (43.5-8008.8)**	19.9 (13.1-32.7)	**83.0 (20.4-315.3)**
K1	46421 (30470-53894)	31131 (15048-77386)	13.0 (5.8-34.7)	**419.0 (40.9-5192.5)**	5.5 (4.0-8.0)	**76.4 (13.7-365.4)**